Bulletin of the Seismological Society of America, Vol 72, No 2, pp 371–387, April 1982

THE ENERGY RELEASE IN EARTHQUAKES

By M. S. Vassiliou and Hiroo Kanamori

ABSTRACT

Energy calculations are generally made through an empirical application of the familiar Gutenberg-Richter energy-magnitude relationships. The precise physical significance of these relationships is somewhat uncertain. We make use here of the recent improvements in knowledge about the earthquake source to place energy measurements on a sounder physical basis. For a simple trapezoidal far-field displacement source-time function with a ratio x of rise time to total duration T_0, the seismic energy E is proportional to $[1/x(1-x)^2]M_0^2/T_0^3$, where M_0 is seismic moment. As long as x is greater than 0.1 or so, the effect of rise time is not important. The dynamic energies thus calculated for shallow events are in reasonable agreement with the estimate $E \cong (5 \times 10^{-5})M_0$ based on elastostatic considerations. Deep events, despite their possibly different seismological character, yield dynamic energies which are compatible with a static prediction similar to that for shallow events. Studies of strong-motion velocity traces obtained near the sources of the 1971 San Fernando, 1966 Parkfield, and 1979 Imperial Valley earthquakes suggest that, even in the distance range of 1 to 5 km, most of the radiated energy is below 1 to 2 Hz in frequency. Far-field energy determinations using long-period WWSSN instruments are probably not in gross error despite their band-limited nature. The strong-motion record for the intermediate depth Bucharest earthquake of 1977 also suggests little teleseismic energy outside the pass-band of a long-period WWSSN instrument.

1. Introduction

The energy released in earthquakes can be estimated in a number of ways (for a comprehensive review see Bath, 1966). We may divide the energy estimates from the variety of methods available into two broad classes: the static estimates and the dynamic estimates. Static estimates can be obtained from static values of moment and stress drop; dynamic estimates, on the other hand, are obtained from seismograms.

We review static estimates of energy in section 4. We discuss there that with some simple assumptions, a static estimate of energy can be obtained from the formula $E = (5 \times 10^{-5})M_0$ (Knopoff, 1958; Kanamori, 1977).

We may subdivide dynamic estimates of energy from body waves into two groups. One procedure involves the direct integration of an observed waveform at a particular station; another involves integration of an inferred displacement source-time function.

The familiar energy-magnitude relationships of Gutenberg and Richter (1942, 1956a, b) fall into the first category of dynamic methods. These empirical relationships were derived on the basis of a crude approximation to the integral over a group of plane seismic waves passing by a station. The Gutenberg-Richter estimates of energy from M_S agree fairly well with the static estimates mentioned above. This might be expected, as M_S correlates quite well with $\log M_0$ (Kanamori and Anderson, 1975).

In this paper, we develop dynamic energy estimates of the second kind. We apply the theory of Haskell (1964) to compute the energies of several shallow events (section 2), using moments and source-time histories obtained in the last decade

from sophisticated waveform modeling. Since there are fewer studies available on intermediate and deep focus events, we also develop a simplified modeling procedure (section 3) to obtain moments and time functions for such events, and use these to estimate energy in the same way as for shallow earthquakes. The energy estimates we obtain are in a sense direct physical dynamic estimates, as opposed to the more empirical approach represented by the energy-magnitude relations. In section 4, we compare dynamic and static estimates for both shallow and deep events.

Our dynamic estimates contain more high-frequency information than the static ones. They are still made, however, at teleseismic distances, and they are furthermore derived from long-period instruments unable to resolve displacement components of frequency greater than 1 to 2 Hz. It is thus possible that some critical high-frequency information is missing. We address this question in section 5, using high-frequency records obtained close to seismic sources with strong-motion instruments.

Finally, in section 6, we compare our dynamic energy estimates with estimates from the Gutenberg-Richter energy-magnitude relations, using M_S for the shallow earthquakes and *long-period* body wave magnitude m_B for the deep and intermediate ones.

2. Dynamic Energy from Source-Time Function

A milestone in the understanding of energy radiation from earthquakes was the paper by Haskell (1964). We essentially follow his treatment, with minor modifications, to obtain expressions for energy release in terms of parameters obtainable from body wave modeling of earthquakes. The important parameters are the seismic moment and the duration and shape of the far-field source-time function. The earthquake displacement observed at far field is given by

$$u(r, t) = [R(\theta, \phi)/4\pi\rho v^3 r]M_0 T(t) \tag{1}$$

where $R(\theta, \phi)$ is a geometric factor accounting for the radiation pattern of the seismic waves; ρ, v, and r are respectively, density, elastic wave velocity, and distance to the source; M_0 is the seismic moment, and $T(t)$ is the far-field source-time function, which is normalized to unit area. This expression assumes that we have already accounted for the effects of attenuation, instrument, receiver structure, and geometric spreading (e.g., Langston and Helmberger, 1975). In the simple case of a one-dimensional rupture with a ramp function, near-source dislocation history, T will generally be trapezoidal in shape (with a triangle as a special case). The trapezoid is obtained by convolving the point-source boxcar (which the near-field ramp produces at far field) with another boxcar representing source finiteness. Other shapes are certainly possible, although not always resolvable by the data. To calculate the energy associated with (1), we begin with a general form of Haskell's (1964) equations (15) and (16)

$$E = \rho v \int_{-\infty}^{\infty} \int_{0}^{2\pi} \int_{0}^{\pi} \dot{u}^2 \, dt r^2 \sin\theta \, d\theta \, d\phi. \tag{2}$$

Equation (2) was derived in the case of spherically symmetric radiation by Yoshiyama (1963). Rudnicki and Freund (1981) derive it for a more general radiation pattern by imposing plane wave conditions at far field. We apply equation (2) separately to P and S waves. We use (1), with $R(\theta, \phi)$ factors appropriate (Haskell,

1964) for a double-couple source, and work the geometric integrals out analytically; adding the P and S wave energies together, we then obtain

$$E = KM_0^2 I_t \tag{3}$$

with

$$K = [(1/15\pi\rho\alpha^5) + (1/10\pi\rho\beta^5)]$$

and

$$I_t = \int_{-\infty}^{\infty} \dot{T}^2(t)\, dt$$

where α and β are the compressional and shear wave velocities. In the earth, $\beta \cong \alpha/\sqrt{3}$, so that the second term in K is dominant, and total energy is approximately equal to shear wave energy. We note that following Plancherel's theorem (Bracewell, 1978), (3) can be written as

$$E = KM_0^2 I_f \tag{4}$$

where

$$I_f = 2\int_0^{\infty} |\dot{T}^{\sim}(f')|^2\, df'$$

and $\dot{T}^{\sim}(f)$ is the Fourier transform of $\dot{T}(t)$. (T is real.)

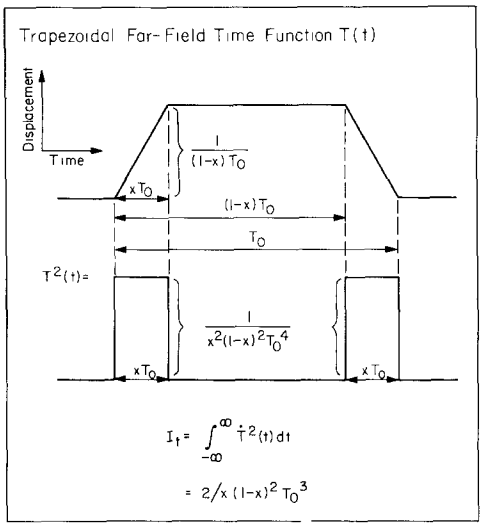

FIG. 1. Trapezoidal far-field displacement time function. Total duration is T_0, rise time is xT_0.

Consider now a simple symmetric trapezoidal far-field time function with a ratio of rise time to total duration represented by x (Figure 1). In this case, the integral

in (3) reduces to

$$I_t = 2/[x(1 - x)^2 T_0^3] \tag{5}$$

where T_0 is total duration. Hence, we have the important result that energy is proportional to the square of the moment, and inversely proportional to the cube of the duration. If one examines the function $1/x(1 - x)^2$, one can easily see that the effect of x is not important unless x is very small, i.e., trapezoidal time functions with x between ~0.1 and 0.5 have roughly the same energy (Figure 2). When functions have very short rise times, this corresponding to the presence of higher frequency components, an appreciable error in the energy can be incurred from even small errors in the rise time. Extremely short rise times are not, however, generally supported by the data, and simple but convincing scaling arguments (Kanamori,

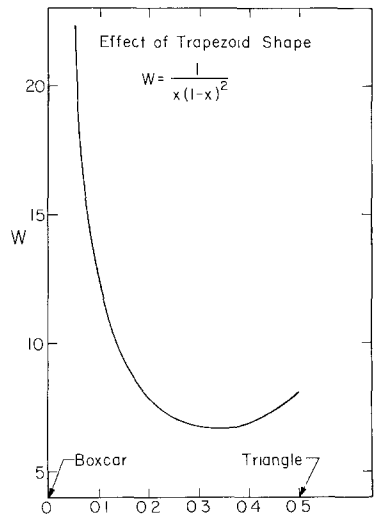

FIG. 2 Effect of trapezoid rise time on calculation of dynamic energy release [see equation (5)]. As long as x (rise time divided by total duration) is greater than 0.1 or so, the effect is not important.

1972; Geller, 1976) lead one to expect values of x greater than 0.1 or so. Hence, we effectively have two important parameters in the energy calculation—the total moment and the total duration. We might note here that the rather artificial presence of sharp corners in the trapezoidal time function does not have an important effect on the total energy. The corners arise from the assumption of a one-dimensional rupture. A fault rupturing along its width as well as its length can be modeled by convolving the point-source far-field boxcar with two boxcars representing finiteness instead of one, this leading to a far-field time function with rounded corners (e.g., Mikumo, 1971, Figure 2). The main shape effect is still due to the rise time, and the above arguments apply.

We may use (3) to calculate the energies of some shallow events for which time functions and moments have been published. Table 1 shows the results of such calculations, which will be discussed in more detail in section 4.

3. A Simplified Procedure for Modeling Deep Focus Events

Waveform modeling can be an extremely time-consuming task; the data shown in Table 1 represent a very large amount of work on the part of many investigators. To obtain a larger data base, one may resort to a more simplified procedure which is

still sufficiently accurate for the purposes of energy computation. The procedure we use is applicable to deep and intermediate events with comparatively simple sources. It consists essentially of estimating the duration of the time function of a simple source from the average pulse width of long-period WWSSN vertical P waves (Bollinger, 1968; Chung and Kanamori, 1980), and then using the average amplitude to infer the moment. We use several stations ($\geqq$10), as well distributed as possible, to average out the effects of radiation pattern and directivity. When the long-period P wave is a single pulse and there are no contaminating free-surface phases, this

TABLE 1

ENERGY CALCULATIONS FOR SOME MODELED SHALLOW EVENTS

Event	Date	log M_0 (dyne-cm)	T_0 (sec)	log E (erg)	M_S	Reference
Oroville	1975	24.8	3	19.7		Langston and Butler, 1976
Truckee	1966	24.8	3	19.7	5.9	Burdick, 1977
Friuli	5/16/76	25.5	4.5	20.5	6.5	Cipar, 1980
Friuli	9/15/76 9/21/76	24.7	4.0	19.2	6.0	Cipar, 1980
Friuli	9/15/76 3/15/76	25.0	3.5	19.9	5.9	Cipar, 1981
Koyna	1967	25.5	6.4	20.2	6.4	Langston, 1976
El Golfo	1966	25.7	4	21.3	6.3	Ebel *et al.*, 1978
Borrego Mt.	1968	26.0	5	21.8	6.9	Burdick and Mellman, 1976
Puget Sound	1965	26.2	3	22.7		Langston and Blum, 1977
Gazli	1976	26.2	8	21 4	7.0	Hartzell, 1980
Haicheng	1975	26.5	7	22.0	7.4	Cipar, 1979
Solomon Is.	1975	27.1	10	22.7	7.7	Lay and Kanamori, 1980
Solomon Is.	7/14/71	28 1	14	24.2	7.9	Lay and Kanamori, 1980
Solomon Is	7/26/71	28.3	16	24.4	7.9	Lay and Kanamori, 1980
	4/16/65	25.1	3.4	20.5		Liu and Kanamori, 1980
	9/4/63	25.2	2.5	21.2		Liu and Kanamori, 1980
	10/23/64	25.8	2.5	22.3		Liu and Kanamori, 1980
	9/30/71	24 9	1.6	21.0		Liu and Kanamori, 1980
	3/24/70	25.2	2.5	21.0		Liu and Kanamori, 1980
Mexico	11/29/78	27.3	15	22.6	7.8	Stewart *et al.*, 1981
Mexico	8/23/65	27.3	16	22.5	7.6	Chael and Stewart, 1982
Mexico	8/2/68	26.9	16	21.7	7.1	Chael and Stewart, 1982
Mexico	3/14/79	27.0	17	22.7	7.6	Chael and Stewart, 1982
Bermuda	3/24/78	25.5	3	21.1	6.0	Stewart and Helmberger, 1981
Gibbs	1967	26.3	17	20.5	6.5	Kanamori and Stewart, 1976
Gibbs	1974	26.7	22	20 9	6.9	Kanamori and Stewart, 1976

method can be quite accurate. When we applied it to the deep and intermediate events studied by Chung and Kanamori (1980), our results for moment and time function were in good agreement with theirs.

To estimate the moment and duration, we use curves of the type shown in Figures 3 and 4 (see legends). These are obtained from synthetic seismograms which are generated by convolving source functions with an instrument response and an attenuation filter. We generally assume that the time function is a trapezoid with $x = 0.2$ (as we have seen, such a trapezoid does not have a significantly different energy from that of a triangle or any trapezoid with $x \geqq 0.1$), and $T^* = 0.7$ in the

attenuation filter (e.g., Chung, 1979). Optimistically, this method, allowing for differences in time function shape, attenuation, etc., can give us an estimate of total duration accurate to ~20 per cent, and an estimate of moment perhaps accurate to within a factor of 2, given the scatter in amplitude due to receiver and other effects. The energy estimate is probably good to an order of magnitude or so. Energies calculated for deep and intermediate events studied by this method, including the events of Chung and Kanamori (1980), are listed in Table 2.

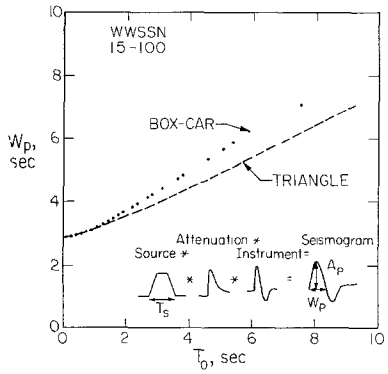

FIG. 3 The relation between measured pulse width W_p of direct vertical P waves on a long-period WWSSN seismogram and the duration T_0 of the far-field source displacement time function (adapted from Chung and Kanamori, 1980) The curves are obtained by convolving the time function with an instrument response and an appropriate Q filter ($T^* = 0.75$ shown here). The curves are reliable provided the P arrival is a single pulse (i.e., the event is simple). In this case, the event is assumed to be deep enough that the direct P wave is not contaminated by free-surface phases.

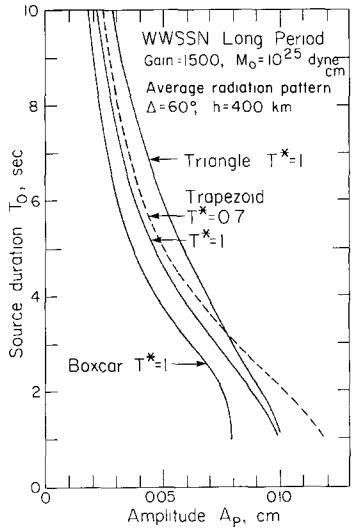

FIG. 4 Examples of curves from which the moment M_0 can be determined for a simple event once the duration T_0 of the far-field time function has been determined For a source depth of 400 km, a source-station distance of 60°, and a peak instrument gain factor of 1500, a curve on this diagram shows the variation of amplitude A_p of direct P on a long-period seismogram with duration of the time function if the moment of the event is 10^{25} dyne-cm Thus for a given T_0, one can read off the expected amplitude for $M_0 = 10^{25}$ dyne-cm, and compare this with the average of amplitude measurements actually made to obtain the moment of the event (corrections are easily made to the amplitude measurement to standardize it to a distance of 60° if necessary). Since an average amplitude measurement is used, the curves drawn here are for an average value of the radiation pattern. The trapezoid function referred to in the figure has a rise time equal to $\frac{1}{3}$ its total duration, which is what we generally assume for events we are studying by this method. The curves drawn for the limiting cases of a boxcar and a triangle show what errors might be incurred if this assumption is unwarranted As can be seen, these errors, as well as those due to uncertainties in attenuation, are probably quite negligible compared to errors due to scatter in amplitudes caused by receiver and other effects

4. Comparison with Static Energy Estimates

We now examine the results of the energy calculations in the framework of an important independent method of estimating energy, based on elastostatic considerations. Consider a simple model of an earthquake where σ_0, σ_1, and σ_f are initial, final, and dynamic frictional stresses on the fault. We may write (Savage and Wood, 1971)

$$W = [(\sigma_0 + \sigma_1)/2 - \sigma_f]DS \tag{6}$$

TABLE 2

Energies Calculated for Intermediate and Deep Focus Events Studied by Means of Simplified Procedure

Origin Time					Region	Depth (km)	m_B	log M_0 (dyne-cm)	T_0 (sec)	log E (erg)
M	D	Y	HMn	Sec						
03	11	68	0826	32 8	Tonga-Kermadec	112	6.2	25.9	4.6	20.7*
08	12	67	0939	44 3	Tonga-Kermadec	134	6.5	26.1	3.7	21.4*
12	08	65	1805	25.2	Tonga-Kermadec	156	6.0	25.4	3.9	20.0*
05	01	69	1905	24.5	Tonga-Kermadec	205	6.1	25 4	2.7	20.5*
03	18	65	1805	25.2	Tonga-Kermadec	219	6.0	25 6	4.7	20.1*
09	04	67	0351	58.9	Tonga-Kermadec	231	6.2	25.8	1.5	22.1*
09	26	68	1437	46.2	Tonga-Kermadec	251	6 0	25.3	2.0	20.6*
06	04	74	0414	13.8	Tonga-Kermadec	256	6.3	26.4	4.7	21.7*
02	22	75	2204	33 5	Tonga-Kermadec	333	6.6	26.5	4.6	21.9*
01	20	68	2121	31.6	Tonga-Kermadec	349	6.0	25.6	1.3	21.8*
07	21	73	0419	13 7	Tonga-Kermadec	373	6.1	25.8	2.8	21.1*
05	27	70	1205	08.3	Bonin Is.	406	6.6	27.0	5.9	22.4
11	18	65	2000	19.5	Tonga-Kermadec	424	6 2	25.6	1.75	21.1*
11	29	74	2205	23.5	Japan	429	6.5	26 6	5 1	21.6
02	03	76	1227	30.1	Tonga-Kermadec	477	6.0	25.8	2.9	20.7*
03	23	74	1428	33.0	Tonga-Kermadec	504	6.3	26.6	4 95	21.6
01	29	71	2158	03.2	Japan	515	6.6	26.8	4.45	22.2
12	28	73	0531	03.8	Tonga-Kermadec	517	6.5	26.2	2.7	21.5
10	25	73	1408	58 5	S. America	517	6.3	25.9	2.2	21.3
10	07	68	1920	20 8	Japan	518	6.7	27.3	13.0	23.4
01	28	66	0436	45.3	Tonga-Kermadec	545	5.8	25.3	1.75	20.3*
01	24	69	0233	03.4	Tonga-Kermadec	587	6.7	26.1	0.75	23.1
06	28	70	1109	51.3	Tonga-Kermadec	587	6 1	25 7	2.35	20 9
07	21	66	1830	15.3	Tonga-Kermadec	590	5.8	25.8	1.8	21.3*
02	15	67	1611	11.8	S. America	598	6.4	26 3	4.1	21 3
10	09	67	1721		Tonga-Kermadec	605	6 8	27.0	4.9	22.4
03	24	67	0900	20.0	Java	601	6.3	26.1	4.1	20.9
03	17	66	1550	33.1	Tonga-Kermadec	630	6.2	26.5	4.0	21 6*
10	01	72	2349		Philippines	632	5.8	25.0	0.7	21.0
02	10	69	2258	03.3	Tonga-Kermadec	635	6.4	25.6	5.2	21.7
12	09	65	1312	55.3	Tonga-Kermadec	649	5.7	25.7	1.8	21.2*

* Events studied by Chung and Kanamori (1980).

where W is the difference between the strain energy drop and the frictional energy, D is the average dislocation, and S is the slip area. By using the stress drop $\Delta\sigma = \sigma_0 - \sigma_1$ and the seismic moment $M_0 = \mu DS$, we can rewrite (6) as

$$W = [\Delta\sigma/2\mu + (\sigma_1 - \sigma_f)/\mu]M_0. \tag{7}$$

Orowan (1960) proposed a physically very reasonable model of a fault whereby motion stops when the accelerating stress decreases to a value equal to some average

dynamic frictional stress, i.e., $\sigma_1 = \sigma_f$. There is thus no overshoot arising from, say, the inertia of the moving fault blocks. In Orowan's model, equation (6), which is the strain energy drop less the frictional energy, represents the energy radiated as seismic waves. If Orowan's condition is satisfied, then clearly the second term in (7) vanishes, and we have simply

$$W = \Delta\sigma M_0/2\mu. \tag{8}$$

Kanamori (1977) used this relationship to estimate the energy released in great shallow earthquakes. With $\Delta\sigma \simeq 20$ to 60 bars, ($\equiv 2$ to 6×10^7 dyne/cm^2), and $\mu \simeq 3$ to 6×10^{11} dyne/cm^2,

$$W_0 \simeq (5 \times 10^{-5})M_0 \tag{9}$$

where we have now adopted the subscript 0 to indicate that this is a static or essentially zero frequency estimate of energy, as opposed to the higher frequency estimates made from (3).

Figure 5 shows a plot of energy versus moment for the shallow events of Table 1.

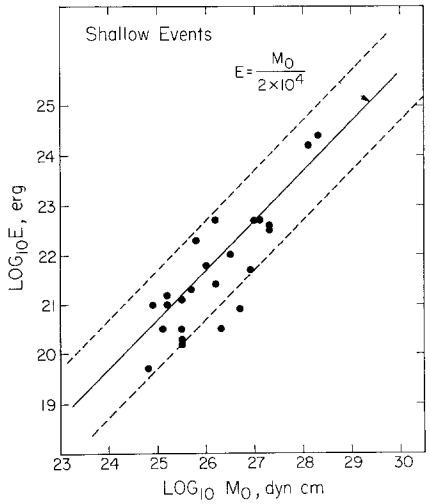

FIG. 5. Energy calculated for some modeled shallow events (Table 1) plotted against seismic moment The line shown corresponds to the approximate relation $E = M_0/(2 \times 10^4)$ (which assumes a stress drop of 20 to 60 bars) obtained by Kanamori (1977). The parallel lines bound an order of magnitude up and down. Considering that this simple elastostatic calculation is completely independent of the dynamic calculations made here from body waves, the agreement is encouraging (see section 4).

The line shows the energy according to (9), with parallel lines bounding an order of magnitude up or down. There is considerable scatter. Some of this scatter must be due to the errors in T_0 and M_0. Another contributing factor, however, probably arises from the fact that (9) is derived assuming $\Delta\sigma$ is 20 to 60 bars, and for many events this obviously need not be true. The dynamic estimates by their very nature take into account the details of rupture for the individual events. For this reason, they can deviate considerably from the line $E = (5 \times 10^{-5})M_0$, perhaps even more than would a crude estimate from M_S. An interesting case is that of the two Gibbs fracture zone events (Kanamori and Stewart, 1976). They lie considerably below the line. As they are known to have been especially slow events, it should not be surprising that (9) might overestimate their energy.

All in all, considering the simplicity of the model leading to the static estimate,

the errors in the dynamic estimate arising from errors in M_0 and T_0, and the independence of the two methods, the agreement between the static and dynamic energy determinations for shallow earthquakes is rather good. We may examine this rough equality more closely by considering some simple static stress-drop scaling relations. In the case of constant stress drop, we may write the moment in terms of stress drop and fault area as (Kanamori and Anderson, 1975)

$$M_0 = \Delta\sigma S^{3/2}. \tag{10}$$

Using an approximate expression $T_0 \cong \sqrt{S}/\beta$ for the time function duration, we obtain

$$M_0 \cong \Delta\sigma\beta^3 T_0^3. \tag{11}$$

Substituting this into (3), and using (5), we have

$$E \cong [2K/x(1-x)^2]\Delta\sigma\beta^3 M_0. \tag{12}$$

Using $x = 0.2$, $\beta = 3.4$ km/sec, $\Delta\sigma = 30$ bars, and $\rho = 2.8$ gm/cm^3 in K gives us

$$E \cong (4.6 \times 10^{-5})M_0 \tag{13}$$

which is very close to (9).

Figure 6 shows energy versus moment for the deep and intermediate events listed

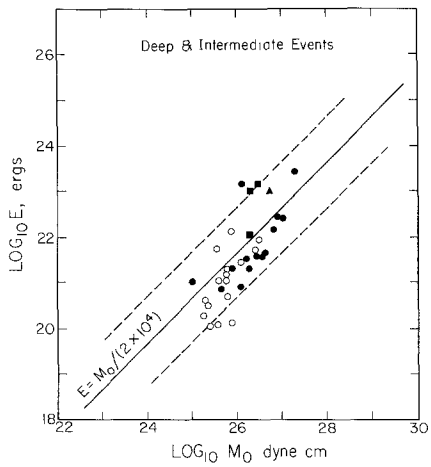

FIG. 6 Similar to Figure 5, but for deep and intermediate events. Circles are for events in Table 2; open circles in particular are for events also studied by Chung and Kanamori (1980), and closed ones are for the rest Closed squares, Mikumo, 1971, closed triangle, Fukao, 1970.

in Table 2. The lines are the same as the ones in Figure 5. On the whole, the deep events tend to plot below the line corresponding to $W_0 = (5 \times 10^{-5})M_0$. Of course, given that our energies are not likely to be accurate to better than an order of magnitude, this may not be significant. However, the effect is quite systematic, and contrary to what one might expect if one believed that deep events tend to have higher stress drops: the average stress drop determined by Chung and Kanamori (1980) for their deep and intermediate events is ~500 bars. If $\mu \cong 6$ to 10×10^{11} dyne/cm^2 below 400 km, the relation $W \cong (5 \times 10^{-5})M_0$ would require $\Delta\sigma \sim 60$ to

100 bars, so if one believed the high stress drops of Chung and Kanamori (1980), one would expect at least the events they studied (we have not determined stress drop for the extra events we studied) to plot above the line.

The key to understanding this situation may lie in remembering that for (8) to hold, Orowan's condition must be met, and this need not be the case. If we assume that the condition is met, we may solve (8) for $\Delta\sigma$, and use values of moment and dynamic energy to obtain a value of stress drop which we may call "Orowan stress drop." This value should be equal to the actual stress drop if Orowan's condition is met; if not, it should be lower. If we calculate Orowan stress drops for the events of Chung and Kanamori (1980), we find that they are considerably lower (Figure 7) than Chung and Kanamori's teleseismically calculated stress drops (using inferences of fault area from the source-time functions). If we calculate the Orowan stress drops using energy determined from m_B (see section 6) instead of our dynamic

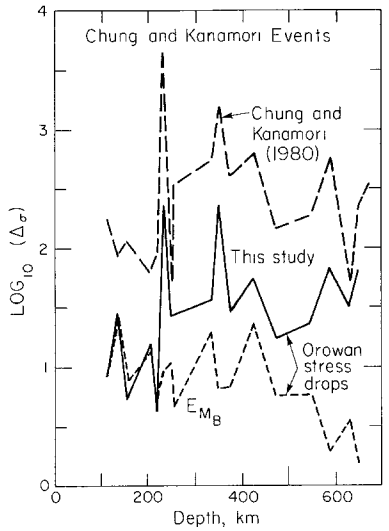

FIG. 7 Upper dotted line = stress drops obtained by Chung and Kanamori (1980) (using source dimensions inferred from far-field time functions), plotted against depth Lower dotted line = "Orowan stress drops," calculated from equation (8) assuming Orowan's condition is met and using energies obtained from m_B. Solid line = "Orowan stress drops" calculated from equation (8) assuming Orowan's condition is met and using dynamic energies calculated in this study. The use of our energies, which are generally higher than those estimated from m_B, does not close the gap between the Orowan stress drops calculated from (8) and those obtained by Chung and Kanamori (1980). Either: (1) our energies are systematically too low; or (2) Chung and Kanamori's (1980) stress drops are too high; or (3) Orowan's condition is not met for these deep and intermediate events.

estimates from section 2, the gap is even wider. The implication then, is that either Orowan's condition is not met for these events, or the condition is met and the Chung-Kanamori stress drops are too high by almost an order of magnitude. Since stress drop is one of the more model-dependent and poorly determined seismological quantities, this would not be too surprising.

In any case, it is not difficult to see why a relationship of the form

$$W = qM_0 \tag{14}$$

can hold for deep and shallow events alike with q approximately given by 5×10^{-5}. From (7) we see that

$$q = [\Delta\sigma/2\mu + (\sigma_1 - \sigma_f)/\mu]. \tag{15}$$

In the case of shallow events, where Orowan's condition is likely to be met (Kanamori and Anderson, 1975), we merely have the reasonable condition, as stated before, that $\Delta\sigma/2\mu \cong 5 \times 10^{-5}$. For deep events, we can have a similar situation as for shallow events, or we can have a non-Orowan process with high stress drops in the first term of (15), and a negative second term.

5. Near-Source Energy Studies and the Question of Frequency Content

The computations which we have carried out are based on earthquake displacement data viewed through a variety of distorting filters, such as attenuation and instrument. We address here the question of the validity of these results, given that by using a long-period instrument we cannot hope to resolve displacement components of frequency greater than 1 to 2 Hz. Beyond the problem of the instrument, we must also consider the possibility that important high-frequency energy is attenuated, either anelastically or through scattering, by propagation of teleseismic distances. One could make the argument that high frequencies observable only very close to the source could be responsible for a considerable portion of the total energy. We note here that we cannot simply quote the fact that teleseismic corner frequencies are relatively low for earthquakes of size similar to the ones examined here as evidence that high frequencies are unimportant. A teleseismic spectrum is not necessarily simply related to the true source spectrum at near-field.

An important source of information with regard to these questions is to be found in near-source strong-motion records. By examining data obtained close ($\leqq$20 km) to the source using high-frequency strong-motion instruments, we can assess the importance of the shorter period energy. From an accelerogram, one can easily obtain a velocity trace, and use that to compute the quantity

$$D(f) = \int_0^f |\dot{u}^{\sim}(f')|^2 \, df' \tag{16}$$

which is proportional to the integral of the energy spectrum to a given frequency; $\dot{u}^{\sim}(f)$ is the Fourier transform of the velocity trace. The seismic wave energy obtained from a trace at a given station is given approximately by

$$E \simeq 4\pi\rho\beta r^2 R(\Theta, \phi)\, 2D(\infty). \tag{17}$$

We note that (16) is not the integral of the source energy density per se, but of the trace energy density. We are thus not looking directly at the true source spectrum. There is some contamination from reflection, refraction, scattering, etc. However, if the high-frequency contribution in traces obtained close to the source is not important, i.e., if D at 2 Hz appears to have already reached a final value, then we can probably not be too worried that we are looking at a trace spectrum rather than a true source spectrum. That is to say, if large amounts of high-frequency energy were present, we might have to be concerned that the contaminating processes we have mentioned might be the origin of it, but if such energy is not there it does not matter as much to our argument that such processes might be present. The contaminating processes we have mentioned would probably, if anything, enhance the high-frequency content of the trace relative to the source, which by itself would argue that if high-frequency energy is negligible in the trace, it must also be negligible in the source. Of course, this ignores attenuation; if we are close enough

to the source, however, attenuation should not be important. We discuss this more fully below.

Figure 8, a to d, shows $D(f)$ for several records from the 1971 San Fernando, 1966 Parkfield, 1979 Imperial Valley, and 1977 Bucharest earthquakes. Table 3 shows values of $D(10)$ and the ratios $D(1)/D(10)$, $D(2)/D(10)$, and $D(4)/D(10)$, where the argument is in Hz, for these and other records. We use $D(10)$ to be essentially representative of $D(\infty)$. This certainly seems justified on inspection of the figures

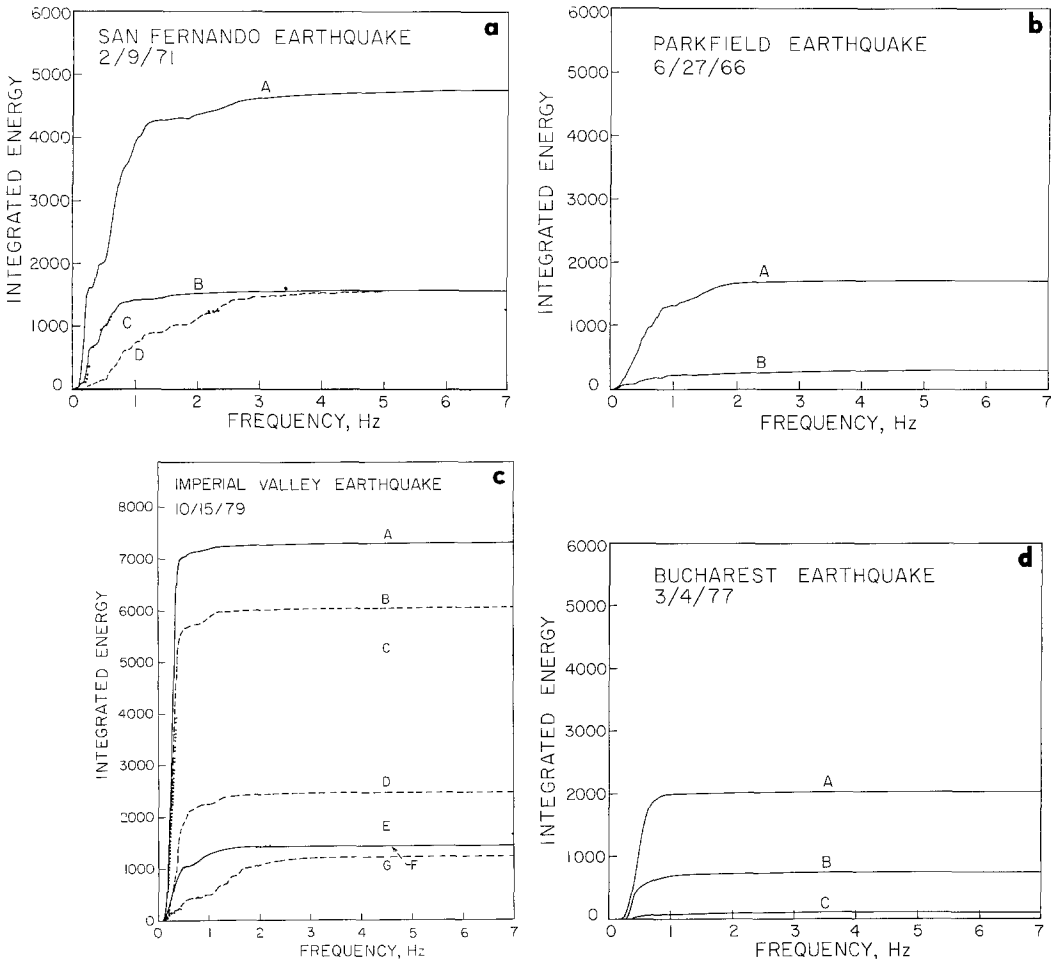

FIG. 8. The integral $D(f)$ (see section 5) of the spectral energy density versus frequency from strong-motion velocity (cm/sec) traces for the San Fernando, Parkfield, Imperial Valley, and Bucharest earthquakes. Different curves for each earthquake correspond to different records (see Table 3) The curves for the San Fernando, Parkfield, and Imperial Valley earthquakes suggest that, even close to the source, by far, most of the energy radiated is below 1 to 2 Hz in frequency. Far-field energy determinations using long-period instruments thus may not be in gross error, despite their band-limited nature.

(in addition, sampling intervals for the digital data are often such that folding frequencies themselves are not much higher than 10 Hz). Many of the records were obtained extremely close to the source [e.g., Pacoima, less than 1 km from the nearest point on the Sierra Madre fault (Heaton, 1982)], and in no case is any appreciable energy observable above 4 Hz. Such energy may exist in the very immediate vicinity of the source, but in that case we may raise semantic questions about which energy to consider "radiated" and which not. If this hypothetical high-

TABLE 3

ENERGY SPECTRAL DENSITY FROM STRONG-MOTION RECORDS (SEE FIGURE 8)

Earthquake	Station	Ref*	Comp	Δ† (km)	$D(10)$‡	$\frac{D(1)}{D(10)}$	$\frac{D(2)}{D(10)}$	$\frac{D(4)}{D(10)}$	Figure and Curve
San Fernando	Pacoima	C041	S16E	~0	4747.3	0.83	0.92	0.99	8a, A
San Fernando	Pacoima	C041	S74W	~0	1590.8	0.47	0 71	0 98	8a, D
San Fernando	Holiday Inn, Orion	C048	N00W	14 5	1575 6	0.89	0.97	1 0	8a, B
San Fernando	Holidav Inn, Orion	C048	S90W	14 5	1425.0	0.95	0 98	1 0	
San Fernando	15250 Ventura Blvd	H115	N11E	21 0	1269 2	0.95	0.97	0.99	8a, C
San Fernando	15250 Ventura Blvd.	H115	N79W	21.0	861.6	0 95	0.96	1.0	
Parkfield	Cholame, Array 2	B033	N65E	22.8, 0.08	1709.1	0 77	0.97	1 0	8b, A
Parkfield	Cholame, Array 5	B034	N85E	23 5, 5.5	311.1	0.72	0.81	0 99	8b, B
Parkfield	Cholame, Array 5	B034	N05W	23.5, 5.5	155.4	0.47	0.72	0.99	
Parkfield	Cholame, Array 12	B036	N40W	27.7, 15.4	122.2	0.96	0.99	1.0	
Imperial Valley	El Centro, Array 6	IIZ004	S50W	24 5, 1.2	7307.5	0.98	0.99	1.0	8c, A
Imperial Valley	El Centro, Array 5	IIZ007	S50W	21.8, 4.0	6056.4	0 97	0 99	1.0	8c, B
ImperialValley	El Centro, Array 7	IIZ003	S50W	24.2, 0 8	5102.0	0.92	1 0	1.0	8c, C
Imperial Valley	El Centro, Array 6	IIZ004	S40E	24.5, 1.2	2470.8	0.91	0.99	1.0	8c, D
Imperial Valley	El Centro, Array 8	IIZ006	S50W	23.9, 3 8	2056 1	0.94	0.98	0.99	
Imperial Valley	El Centro, Array 5	IIZ007	S40E	21 8, 4.0	2022.0	0.91	0.97	0.99	
Imperial Valley	El Centro, Bonds Corner	IIZ005	S50W	3.7	1641.4	0.43	0.86	0.98	8c, E
Imperial Valley	El Centro, Array 8	IIZ006	S40E	23.9, 3 8	1499.9	0.91	0.97	0 99	
Imperial Valley	El Centro, Array 7	IIZ003	S40E	24 2, 0.8	1442.9	0 89	0 99	1.0	8c, F
Imperial Valley	El Centro, Bonds Corner	IIZ005	S40E	3.7	1230.6	0.41	0 86	0 98	8c, G
Bucharest	Bld. Res Inst.		S-N	190	2029.2	0.98	1.0	1.0	8d, A
Bucharest	Bld. Res. Inst.		E-W	190	743.0	0.88	0.99	1.0	8d, B
Bucharest	Bld. Res. Inst.		U-D	190	88.9	0 84	0.96	0.99	8d, C

* Reference number of accelerogram in CalTech Earthquake Engineering Research Laboratory Reports.

† Where two distances are given, the first is that to the epicenter, and the second is that to the nearest point of the fault.

‡ $D(f) = \int_0 |\dot{u} \sim (f')|^2 \, df'$, where f is frequency in Hertz $D(10)$ is taken to represent $D(\infty)$. $\dot{u}^N(f)$ is the Fourier transform of $\dot{u}(t)$, and $u(t)$ is in centimeters/seconds.

frequency energy is attenuated within 1 km of the source, we might perhaps not consider it to be radiated energy, but rather some form of frictional energy. This reasoning applies also to energy at 1 to 2 Hz. If there is important energy in this band which we cannot see even at 1 km or so from the fault (actually, with a Q of about 300 this is unlikely), then we can hardly worry about it for the purposes of computing *radiated* seismic energy.

What we have set out to do in examining the strong-motion records is to see if there was a large proportion of energy there which we were missing at teleseismic distances. It is clear from the records presented here that even very close to the source, by far the largest proportion of the energy is contained in frequencies below 2 Hz. In many cases, over 90 per cent of the energy is even below 1 Hz. What these results suggest is that no appreciable error (certainly not one of an order of magnitude) is incurred by making an energy determination at far field using a long-period instrument.

Strictly, this only applies to shallow events. Certainly we have no instances of strong-motion recordings within 1 km of the source of a deep focus event, so we cannot directly address the problem of whether ther is important energy within a few kilometers of the source which never propagates out to teleseismic distances. We can, however, make some statement about whether or not a long-period instrument is broad enough in its frequency response to retrieve adequately the energy that does manage to propagate to the teleseismic range. The curves of Figure 8d for the 100-km depth Bucharest earthquake in fact show very little energy outside the passband of a long-period WWSSN instrument (~60 sec to 1 to 2 Hz), and this is encouraging.

6. Energy and Magnitude

In this section, we compare our dynamic energy estimates with the energies one would obtain using the Gutenberg-Richter relations. For the shallow events of Table 1, the comparison is relatively straightforward; we may use M_S as a measure of magnitude. Figure 9a shows log E in ergs versus M_S for these events. Our estimates seem to be consistently lower than the Gutenberg-Richter line. A best-fit line through our points would have slope 1.81(±0.2) and intercept 9.06(±1.38), compared to 1.5 and 11.8, respectively, for Gutenberg-Richter.

The comparison for the deep and intermediate events of Table 2 is more ambiguous. These events generally did not excite appreciable surface waves, so we must use a body-wave magnitude. Gutenberg and Richter derived the relation $\log_{10} E = 2.4m_B + 5.8$. The magnitude m_B is not the same as the m_b now in common use. The latter is a short-period (~1-sec) body-wave magnitude, while the former is a longer period one. We have used long-period WWSSN records to determine an m_B more compatible than m_b with Gutenberg and Richter's definition.

One difficulty which arises is that when the P wave consists essentially of a single pulse, as is the general case with the simple events we have studied here, the measurement of the dominant period in the wave group becomes ambiguous. We have set the period to twice the pulse width. Another difficulty is that the WWSSN instruments whose records we have employed are peaked at 15 sec, while Gutenberg and Richter used mechanical instruments with a different period response (flat rather than decaying); thus, one must be careful to use the correct gain for the WWSSN instrument when one is looking at a period different from the peak period. The waveforms from the two instruments differ; we have conducted some numerical experiments to ascertain that no drastic errors occur because of this.

A plot of log E versus m_B for the intermediate and deep events of Table 2 is shown in Figure 9b. In contrast to the case of the shallow events, the bias here is above the Gutenberg-Richter line. The least-squares line through our plotted points has slope 1.97(±0.34) and intercept 9.07(±2.13). We note that if one allows an error of 0.5 units in m_B, taking into account all the factors mentioned above, as well as an error of an order of magnitude in the energy, the discrepancy is understandable.

Although it is interesting that the shallow events generally plot below the log E − M_S line, while the deep and intermediate ones plot above the log E − m_B line, we

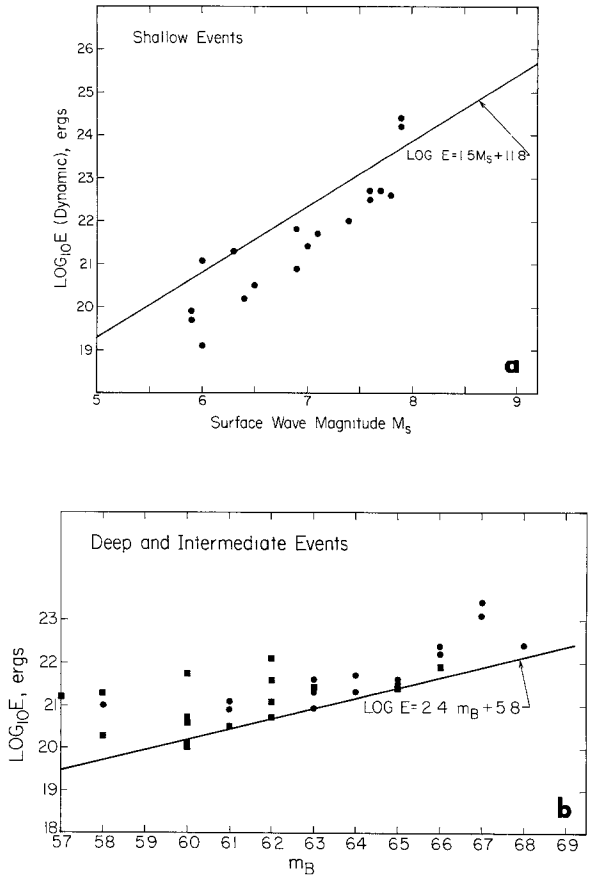

FIG 9. (a) Common logarithm of the dynamic energy release in ergs plotted against M_S for shallow events of Table 1. The line represents the Gutenberg-Richter relationship. (b) Common logarithm of the dynamic energy release in ergs plotted against m_B (long-period body-wave magnitude—see section 6) for the deep and intermediate events of Table 2 Squares represent events also studied by Chung and Kanamori (1980). The line represents the Gutenberg-Richter relationship.

cannot really make meaningful comments about this given the empirical nature of the Gutenberg-Richter relationships.

7. CONCLUSIONS

1. The important parameters in the calculation of seismic energy release from body waves are seismic moment M_0 and far-field displacement time function duration T_0, with $E \sim M_0^2/T_0^3$. The important shape effect for the usual trapezoidal time function comes from its ratio x of rise time to total duration. As long as $x \geqq 0.1$, which is generally supported by the data, the effect is not important.

2. Our near-source studies suggest that most of the important radiated energy is below 1 to 2 Hz in frequency, and hence that far-field energy determinations using long-period WWSSN instruments are not in gross error despite their band-limited nature.
3. Dynamic energy estimates for shallow earthquakes made from body waves are in reasonable agreement with expectations from simple static elastic relaxation models, which suggest that $E \cong (5 \times 10^{-5})M_0$ for shallow events when a stress drop of 20 to 60 bars is assumed.
4. Deep events, despite their possibly different seismological character, yield dynamic energies which are also compatible with a static energy prediction similar to that for shallow events. Seismic moment M_0, and hence a moment-based magnitude scale, may reliably be used for shallow and deep events alike, as a reasonably accurate measure of energy release.

Acknowledgments

We thank Medhat Haroun, who was most helpful in providing us with the strong-motion data we needed. Discussions with Bernard Minster and Larry Ruff were helpful. We also thank Tom Heaton, Steve Hartzell, and Jeff Given for reading through the manuscript. This research was supported by the Earth Science Section, National Science Foundation, Grants EAR77-13641 and EAR78-11973.

References

Bath, M (1966). Earthquake energy and magnitude, in *Physics and Chemistry of the Earth*, vol 7, L H. Ahrens, F Press, S. K Runcorn, and H C. Urey, Editors, Pergamon Press, New York, 117–165.

Bollinger, G. A. (1968). Determination of earthquake fault parameters from long period P waves, *J. Geophys. Res.* **73,** 785–807.

Bracewell, R N. (1978). *The Fourier Transform and Its Applications*, 2nd ed., McGraw-Hill, New York.

Burdick, L. J. (1977). Broad band seismic studies of body waves. *Ph.D. Thesis*, California Institute of Technology, Pasadena, California.

Burdick, L. J. and G. R. Mellman (1976). Inversion of body waves of the Borrego mountain earthquake to the source mechanisms, *Bull. Seism. Soc. Am.* **66,** 1485–1499.

Chael, E. and G Stewart (1982). Recent large earthquakes along the middle America trench and their implications for the subduction process, *J. Geophys. Res.* (in press).

Chung, W Y. (1979) Variation of seismic source parameters and stress drop within a descending slab as revealed from body-wave pulse-width and amplitude analysis, *Ph.D. Dissertation*, Seismological Laboratory, California Institute of Technology, Pasadena, California.

Chung, W. Y. and H. Kanamori (1980) Variation of seismic source parameters and stress drops within a descending slab and its implications in plate mechanics, *Phys Earth Planet. Interiors* **23,** 134–159.

Cipar, J. (1979). Source processes of the Haicheng, China, earthquake from observations of *P* and *S* waves, *Bull. Seism. Soc. Am* **69,** 1903–1916.

Cipar, J. (1980). Teleseismic observations of the 1976 Friuli, Italy, earthquake sequence, *Bull. Seism. Soc. Am.* **70,** 963–1983.

Cipar, J (1981). Broadband time domain modeling of earthquakes from Friuli, Italy, *Bull. Seism Soc. Am.* **71,** 1215–1231.

Ebel, J. E., L. J. Burdick, and G. Stewart (1978) The source mechanism of the August 7, 1966 El Golfo Earthquake, *Bull. Seism Soc Am* **68,** 1281–1292.

Fukao, Y (1970). Focal process of a deep focus earthquake as deduced from long period *P* and *S* waves, *Bull Earthquake Res Inst., Tokyo Univ* **48,** 707–727.

Geller, R. J (1976). Scaling relations for earthquake source parameters and magnitudes, *Bull Seism Soc. Am* **66,** 1501–1523.

Gutenberg, B. and C. F Richter (1942). Earthquake magnitude, intensity, energy, and acceleration, *Bull Seism. Soc. Am* **32,** 163–191.

Gutenberg, B. and C. F. Richter (1956a). Earthquake magnitude, intensity, energy, and acceleration (second paper), *Bull Seism. Soc. Am.* **46,** 105–145.

Gutenberg, B. and C. F. Richter (1956b). Magnitude and energy of earthquakes, *Ann. Geofis.* **9,** 1–15.

Hartzell, S. (1980). Faulting process of the May 17, 1976 Gazli, USSR, earthquake, *Bull. Seism. Soc. Am.* **70,** 1715–1736.

Haskell, N. A. (1964) Total energy and energy spectral density of elastic wave radiation from propagating faults, *Bull. Seism. Soc. Am.* **54,** 1811–1841.

Heaton, T. H. (1982). The San Fernando earthquake; a double event (submitted for publication)

Kanamori, H (1972) Determination of effective tectonic stress associated with earthquake faulting, *Phys. Earth Planet. Interiors* **5,** 426–434.

Kanamori, H. (1977). The energy release in great earthquakes, *J. Geophys. Res.* **82,** 2981–2987.

Kanamori, H and D. L. Anderson (1975). Theoretical basis of some empirical relations in seismology, *Bull. Seism. Soc. Am* **65,** 1073–1095.

Kanamori, H. and G. S. Stewart (1976) Mode of the strain release along the Gibbs fracture zone, Mid-Atlantic ridge, *Phys. Earth Planet Interiors* **11,** 312–332.

Knopoff, L. (1958) Energy release in earthquakes, *Geophys. J* **1,** 44–52.

Langston, C. A. (1976). A body wave inversion of the Koyna, India earthquake of December 10, 1967 and some implications for body wave focal mechanisms, *J. Geophys Res.* **81,** 2517–2529.

Langston, C. A. and D. V Helmberger (1975) A procedure for modelling shallow dislocation sources, *Geophys. J.* **42,** 117–130.

Langston, C. A. and R. Butler (1976). Focal mechanism of the August 1, 1975 Oroville earthquake, *Bull. Seism. Soc. Am.* **66,** 1111–1120.

Langston, C. A. and D. E. Blum (1977). The April 29, 1965 Puget Sound earthquake and the crustal and upper mantle structure of western Washington, *Bull. Seism. Soc. Am* **67,** 693–711.

Lay, T. and H. Kanamori (1980) Earthquake doublets in the Solomon Islands, *Phys Earth Planet. Interiors* **21,** 283–304.

Liu, H. L and H. Kanamori (1980). Determination of source parameters of mid-plate earthquakes from the waveforms of body waves, *Bull. Seism. Soc. Am.* **70,** 1989–2004.

Mikumo, T. (1971). Source process of deep and intermediate earthquakes as inferred from long period *P* and *S* waveforms: 1 Intermediate depth earthquake in S.W. Pacific region, *J Phys Earth* **19,** 1–19.

Orowan, E. (1960) Mechanism of seismic faulting, *Geol. Soc. Am Mem* **79,** 323–345

Rudnicki, J. W. and L B. Freund (1981) On energy radiation from seismic sources, *Bull Seism. Soc. Am.* **71,** 583–595.

Savage, J. C. and M. D. Wood (1971). The relation between apparent stress and stress drop, *Bull. Seism Soc. Am.* **61,** 1381–1388.

Stewart, G. S. and D. V. Helmberger (1981). The Bermuda earthquake of March 24, 1978: a significant oceanic interplate event, *J. Geophys. Res.* **86,** 7027–7036.

Stewart, G. S., E. P. Chael, and K. C. McNally (1981). The November 29, 1978 Oaxaca earthquake: a large simple event, *J. Geophys. Res.* **86,** 5053–5060

Yoshiyama, R. (1963). Note on earthquake energy, *Bull. Earthquake Res Inst., Tokyo Univ.* **41,** 687–697.

SEISMOLOGICAL LABORATORY
CALIFORNIA INSTITUTE OF TECHNOLOGY
PASADENA, CALIFORNIA 91125
CONTRIBUTION NO. 3631

Manuscript received 2 June 1981